# Modelling of Transit-Time Ultrasonic Flow Meters Under Multi-phase Flow Conditions

Matej Simurda
and Lars Duggen
Mads Clausen Institute
University of Southern Denmark
Sønderborg, 6400, Denmark
Email: simurda@mci.sdu.dk
Email: duggen@mci.sdu.dk

Benny Lassen
DONG Energy
Denmark

Nils T. Basse
Siemens A/S Flow Instruments
Sønderborg, 6400, Denmark

***Abstract*—A pseudospectral model for transit time ultrasonic flowmeters under multiphase flow conditions is presented. The method solves first order stress-velocity equations of elastodynamics, with acoustic media being modelled by setting shear modulus to zero. Additional terms to account for the effect of the background flow are included. Spatial derivatives are calculated by a Fourier collocation scheme allowing the use of the Fast Fourier transform. The method is compared against analytical solutions and experimental measurements. Additionally, a study of clamp-on and in-line ultrasonic flowmeters operating under multiphase flow conditions is carried out.**

## I. Introduction

Transit-time ultrasonic flowmeters (TTUF) is a family of devices that measure fluid flow rate based on a difference of times it takes an ultrasonic signal to cross the pipe when propagating with and against the flow. There are two main solutions available on the market. In-line flowmeters are manufactured as a spool-piece with embedded transducers that is mounted directly into a pipeline. In clamp-on configuration, transducers are mounted from the outside so the measurement does not affect the flow. As a trade off the signal needs to penetrate through the pipe wall. Moreover, flowing media can consist of two or more substances of very different acoustic impedance so the ultrasonic beam transmits through and reflects from multiple solid-solid, solid-fluid and fluid-fluid interfaces affecting the measurement signal significantly. Numerical simulations are a useful tool for analyzing and possibly accounting for such scenarios.

There have been several approaches published on this matter such as the use of geometrical acoustics [1], [2] which, however do not account for diffraction. Finite difference (FD) [3] and finite element methods (FEM) [4] employ wave theory through solving the linearized Euler equations (acoustic media) or the equations of linear elasticity (solid media). These require a relatively high number of points per minimum wavelengths (PPMW) which can be an issue in terms of computing resources in case of ultrasonic flowmeter simulations where the signal usually propagates over a distance of hundreds of wavelengths. Bezdek *et al.* [5] presented an alternative approach where FEM is only used in the solid parts and a boundary integral method is applied in the flowing part assuming a homogeneous fluid.

In this paper we focus on the propagation of ultrasonic signals in two phase flow where the two substances have a high acoustic impedance mismatch. This is the case for flow measurement of water/air bubbles mixture where the scattering from bubbles affects the measurement accuracy significantly.

The method evaluates spatial derivatives by a Fourier collocation scheme allowing the use of the Fast Fourier transform while a finite difference scheme (the third order Runge-Kutta [6]) is used to advance in time. This approach is sometimes called a pseudospectral time domain (PSTD) [7] method.

After validating the code against analytical solutions, models of in-line and clamp-on ultrasonic flowmeters operating under multiphase flow conditions and study of measurement accuracy are presented.

## II. Governing equations

In this paper, we assume a modified system of first order partial differential equations coupling particle displacement velocity $v_i$ and stress $\sigma_{ij}$ describing propagation of elastic waves in isotropic media [8], [9]

$$\begin{aligned}\frac{\partial \sigma_{ij}}{\partial t} &= \lambda \delta_{ij} \frac{\partial v_k}{\partial x_k} + \mu \left( \frac{\partial v_i}{\partial x_j} + \frac{\partial v_j}{\partial x_i} \right) \\ &- \lambda \delta_{ij} v_{0k} \frac{\partial}{\partial x_k} \left( \frac{\sigma_{ij}}{\lambda} \right), \qquad (1)\\ \rho \frac{\partial v_i}{\partial t} &= \frac{\partial \sigma_{ij}}{\partial x_j} + f_i - \rho v_{0k} \frac{\partial v_i}{\partial x_k} - \rho v_k \frac{\partial v_{0i}}{\partial x_k}, \qquad (2)\end{aligned}$$

where $x_i$, $i = 1, 2, 3$ are Cartesian position coordinates,$\lambda$, $\mu$, $\rho$ and $f_i$ denote the Lamé elastic constant, shear modulus, mass density and body force respectively. In these equations the Einstein summation convention is used and $\delta_{ij}$ is the Kronecker Delta. Acoustic media can be modelled by setting shear modulus $\mu$ to zero and $v_{0k}$ is the background flow velocity that can vary both in time and space but is zero in regions of elastic media.

## III. Numerical method

The Fourier collocation method is implemented in this work to evaluate all derivatives with respect to two dimensional physical space. Consider an arbitrary interval of length $l$ discretized into $N$ evenly distributed points with step size $\Delta x$ ($l = \Delta x N$). The spatial differentiation can be then approximated by [10]

$$\frac{\partial[.]}{\partial x} \approx Re\left(\mathcal{F}^{-1}\left(ik\mathcal{F}(.)\right)\right), \tag{3}$$

where $\mathcal{F}$ and $\mathcal{F}^{-1}$ are the discrete Fourier and inverse Fourier transform of a function $f(x)$ respectively

$$\begin{aligned}\mathcal{F}\left(f(x)\right)(k) &= \hat{f}(k) = \Delta x \sum_{j=1}^{N} f(x_j) e^{-ikx_j},\\ \mathcal{F}^{-1}\left(\hat{f}(k)\right)(x) &= f(x) = \frac{1}{\Delta x N}\sum_{j=1}^{N} \hat{f}(k_j) e^{ik_j x},\end{aligned} \tag{4}$$

and $k$ is the vector of wavenumbers

$$k = \begin{cases} \left[-\frac{N}{2}, -\frac{N}{2}+1, ..., \frac{N}{2}-1\right]\frac{2\pi}{\Delta x N} & \text{if } N \text{ is even} \\ \left[-\frac{N-1}{2}, -\frac{N-1}{2}+1, ..., \frac{N-1}{2}-1\right]\frac{2\pi}{\Delta x N} & \text{if } N \text{ is odd.}\end{cases}$$

Using the Fourier collocation method inherently imposes periodic boundary conditions. In order to suppress waves leaving domain on one side to instantly reappear on the opposite side multi-axial perfectly matched layers(M-PML) [11] are implemented in this work.

Stability and efficiency of the method is improved by implementing spatial staggering such that the stress and the velocity components are evaluated on grids shifted by half of the grid spacing $\Delta x/2$. Temporal staggering is impossible due to the fact that the equations (1),(2) are not interlaced [12] because of the presence of the background flow terms $v_{0k}$.

In this study, we consider fluid mixtures of very high acoustic impedance contrasts. As the Fourier collocation method expresses the solution in basis of trigonometric functions it will inherently develop numerical issues for problems with such strong discontinuities due to the *Gibbs phenomenon*. An alternative approach is therefore taken, where zero values on stress variables are directly imposed at each stage of the time integration which is an acceptable approximation as long as the acoustic impedance of the host medium is several orders of magnitude higher than the acoustic impedance of the second phase. This way we avoid numerical issues that would be associated with a spectral differentiation of mass density.

Finally, the equations are integrated in time with an explicit third order Runge-Kutta scheme [6].

## IV. Test cases

In this section a comparison against an analytical solution is presented and the validity of the above mentioned approach of simulating high contrast agents is discussed. The method is then validated against experimental measurements.

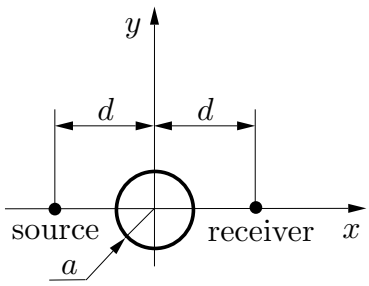


Fig. 1. Cylindrical inclusion in a homogeneous medium. All dimensions are in mm

TABLE I
Parameters of the model of point source in a homogeneous medium with a cylindrical inclusion

| | | |
|---|---|---|
| $d$ | 7 | mm |
| $a$ | 0.65 | mm |
| $\mu_{medium}$ | $2.25 \times 10^9$ | Pa |
| $\rho_{medium}$ | 1024.4 | kg/m$^3$ |
| $\mu_{inclusion}$ | $1.44 \times 10^5$ | Pa |
| $\rho_{inclusion}$ | 1.22 | kg/m$^3$ |
| $\Delta x = \Delta y$ | 0.11 | mm |
| $\Delta t$ | $1.54 \times 10^{-8}$ | s |

### A. Point source in a homogenenous medium with a cylindrical inclusion

We consider shear waves propagating in $x - y$ plane in a homogeneous elastic medium with a cylindrical cavity of radius $a$ centered at the origin. A point source is located at $x_s = d$, $y_s = 0$ and the displacement is recorded at a point $x_r = -d$, $y_r = 0$.

Dimensions are depicted in Figure 1 and all parameters tabulated in Table I where $\Delta t$ represent the time integration step. The material properties are chosen such that shear wave velocities of the host medium and the inclusion match longitudinal velocities of water and air respectively. Considering the high impedance mismatch, the above mentioned approach of assigning zero values on the stress variables at grid points of the cavity was taken in the model. The input signal is a burst of five sine pulses of frequency $f_c$ multiplied by the *Hanning* window.

The simulation results were compared to an analytical solution that was evaluated by numerically convolving Green's function [13] and the comparison for different input signal center frequencies $f_c$ is presented in Figure 2.

The model agrees exceptionally well in the range of low frequencies, but exhibits amplitude discrepancies in the range of shorter wavelengths. This is very likely due to the fact that the cylindrical cavity is approximated on the rectangular grid. It is noteworthy that there seems to be a threshold for the amplitude error, being practically zero at $f_c = 0.5$MHz, but already about $5\%$ at $0.75$MHz and $15\%$ at 1MHz. The discretization length (i.e. distance between grid points) in these simulations was chosen as $0.11$mm. Hence the threshold of circle discretization error is between 27 and 18 PPMW. There is, however, no significant change in the signal envelope,

TABLE II
PARAMETERS OF THE MODEL AND THE EXPERIMENTAL MEASUREMENT SETUP

| | | |
|---|---|---|
| $d$ | 39.4 | mm |
| $l$ | 138.7 | mm |
| $w$ | 16.1 | mm |
| $a$ | 2.05 , 3 , 4 | mm |
| $\lambda_{water}$ | $2.25 \times 10^9$ | Pa |
| $\rho_{water}$ | 1024.4 | $\mathrm{kg/m^3}$ |
| $\Delta x = \Delta y$ | 0.11 | mm |
| $\Delta t$ | $1.54 \times 10^{-8}$ | s |
| $V_{pp}$ | 10 | V |
| $f_c$ | 1 | MHz |

which is essential for transit time ultrasonic flow measurement applications.

### B. Experimental measurements

A measurement setup similar to the test case discussed in the previous subsection was used to verify the model experimentally. Two ultrasonic transducers consisting of a piezoceramic crystal with center frequency $f_c = 1$ MHz coupled to a half-wavelength steel window were immersed in a waterbath directly facing each other. Sealed cylinders of different radii $a$ were manufactured from aluminium foil and used as air phantoms. The foil thickness is declared to be approximately $0.02$ mm and is not included in the model as it is about 75 times smaller than the expected wavelength of 1 MHz signal in water.

The measurement setup is schematically depicted in Figure 3 and parameters tabulated in Table II. An input signal burst of 5 sine cycles with peak-to-peak voltage $V_{pp}$ was generated by the Agilent 33120A Waveform Generator and the received voltage was measured over a $50\ \Omega$ resistor connected in series in the receiver circuit. Maesurements were carried out using Agilent MSO6014A digital oscilloscope and are shown in Figure 4. To transfer from electric signal to stress-velocity variables and back a 1-D transducer model developed by Willatzen [16] was used.

Some parameters of the model such as properties of the piezoceramic material were found by optimizing the error between the measurement and the simulation result for the case of propagation in homogeneous medium. It should therefore come as a no surprise that the curves depicted in Figure 4a are in such a good agreement. The remaining comparisons exhibit some differences in both envelope shape and magnitude. Once the phantom has been introduced, the amplitude mismatch is about 11% which fits fairly well with the error seen in Figure 2c. For the bigger phantom diameters, the amplitudes scale quite similarly, i.e. the scaling factors between cases II,III, and IV are $1.55, 1.57$ for experimental data and $1.36, 1.56$ for our simulation data, respectively. Hence, the difference in amplitude is explained by the bubble discretization discussed in the previous section. The difference in envelope shape is very likely due to the transducer model that assumes the crystal operation in thickness mode. Once an inclusion is placed in the sonic path the resulting pressure on the receiver plane is not

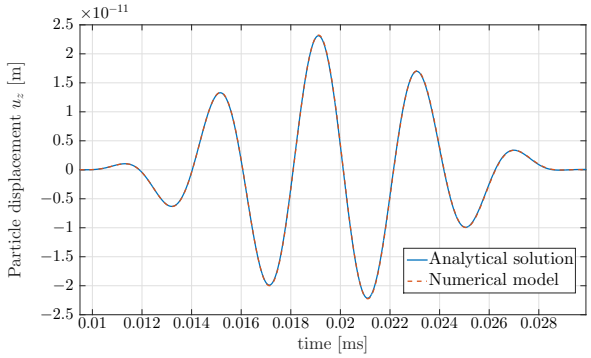


(a) $f_c = 0.25$ MHz

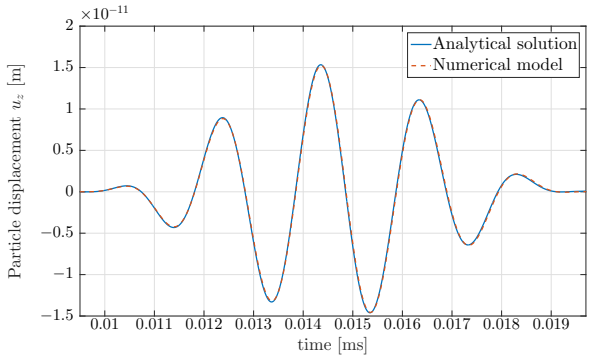


(b) $f_c = 0.5$ MHz

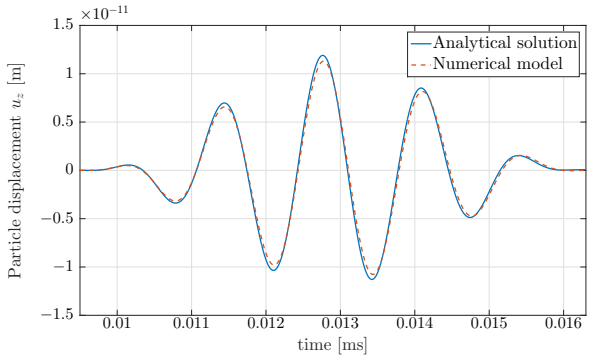


(c) $f_c = 0.75$ MHz

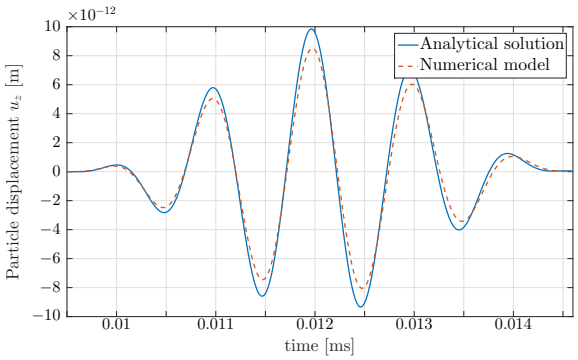


(d) $f_c = 1$ MHz

Fig. 2. Comparison of the experimental measurements and the simulation results

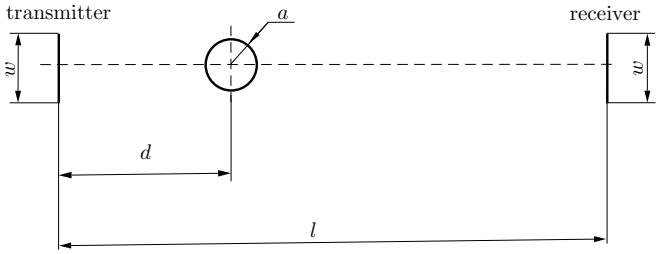


Fig. 3. Cylindrical inclusion in a homogeneous medium. All dimensions are in mm

TABLE III
PARAMETERS OF THE CLAMP-ON MEASUREMENT SETUP

| | | |
|---|---|---|
| $h_w$ | 12 | mm |
| $h_p$ | 3.7 | mm |
| $h_f$ | 13.9 | mm |
| $w$ | 15 | mm |
| $d$ | 3.5 | mm |
| $a$ | 0.8 | mm |
| $\vartheta_w$ | 45 | $^o$ |
| $\lambda_w$ | $4.72 \times 10^9$ | Pa |
| $\mu_w$ | $1.53 \times 10^9$ | Pa |
| $\rho_w$ | 1280 | kg/m$^3$ |
| $\lambda_p$ | $1.12 \times 10^{11}$ | Pa |
| $\mu_p$ | $8.04 \times 10^{10}$ | Pa |
| $\rho_p$ | 7850 | kg/m$^3$ |
| $\lambda_f$ | $2.25 \times 10^9$ | Pa |
| $\mu_f$ | 0 | Pa |
| $\rho_f$ | 1024.4 | kg/m$^3$ |
| $\Delta x = \Delta y$ | 0.14 | mm |
| $\Delta t$ | $4.87 \times 10^{-9}$ | s |
| $f_c$ | 0.77 | MHz |
| $t_{delay}$ | 1 | $\mu$s |

uniform possibly giving rise to transverse waves in the steel window and other than thickness modes in the piezo crystal. Such behaviour cannot be described by the one dimensional transducer model and is therefore very likely the reason for the envelope mismatch.

## V. FLOWMETER SIMULATIONS

In this section a study on impact of the multiphase flow on the accuracy of clamp-on and in-line ultrasonic flowmeters is presented.

The model of a clamp-on flowmeter is depicted in Figure 5 showing a system of layers that represent coupling wedge, pipe, and the flowing fluid respectively. The model parameters are tabulated in Table III. A cluster of four air bubbles is positioned at the center of the pipe with its rightmost bubble lying on the ideal acoustic path and a uniform flow profile with velocity $v_{0x}$ is assumed inside the pipe. The in-line flowmeter is simulated by setting material properties of the coupling wedge and the pipe to be the same as for the fluid and the receiver position is shifted appropriately so that the transducers are acoustically facing each other. The air bubbles are again simulated by setting zero stresses at these grid points. The input signal is a burst of eight sine pulses of frequency $f_c$ multiplied by the *Hanning* window.

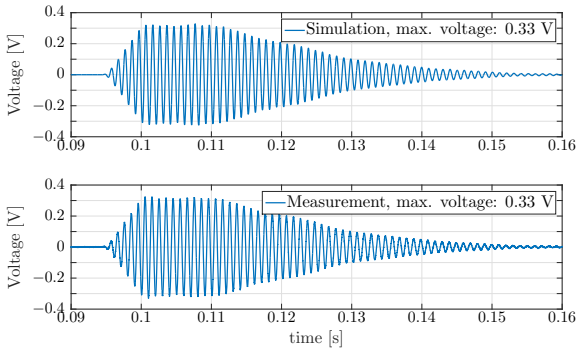


(a) Case I: homogeneous medium

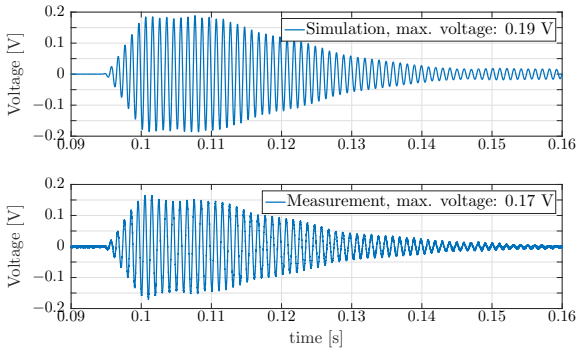


(b) Case II: $d = 4.1$ mm

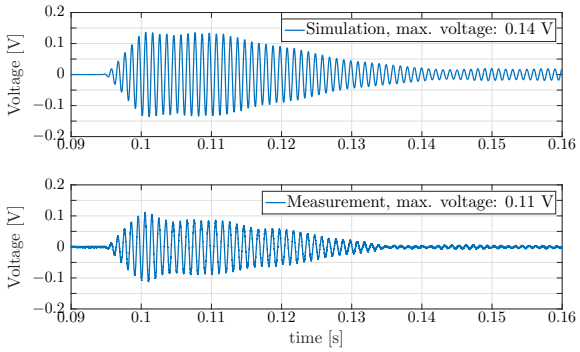


(c) Case III: $d = 6$ mm

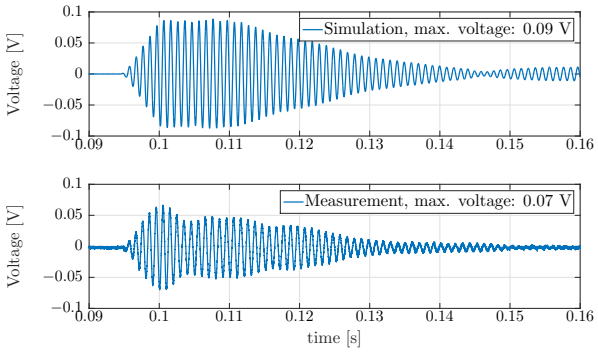


(d) Case III: $d = 8$ mm

Fig. 4. Comparison of the experimental measurements and the simulation results

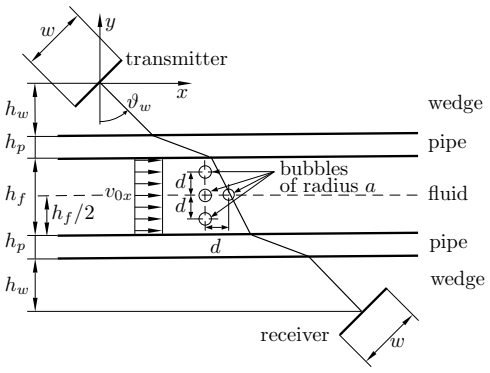


Fig. 5. Clamp-on flowmeter scheme

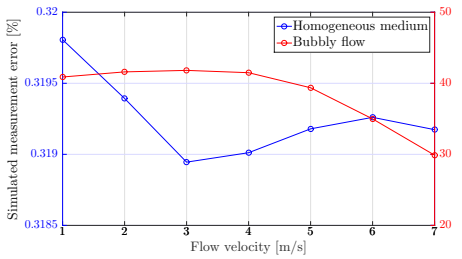


Fig. 6. Comparison of clamp-on flowmeter simulated measurement error for homogeneous medium and bubbly flow

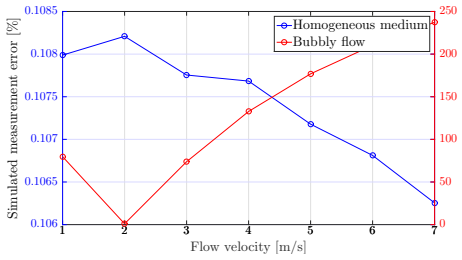


Fig. 7. Comparison of in-line flowmeter simulated measurement error for homogeneous medium and bubbly flow

For each background flow velocity the propagation of the signal in the downstream direction is calculated. The bubbles are then shifted in $x$ direction by a distance $x_{delay} = v_{0x}t_{delay}$ where $t_{delay}$ represents a delay between the upstream and downstream measurement. The upstream propagation is then simulated and the transit time difference is calculated by cross correlating up- and downstream received signals and the measurement error is subsequently determined using the standard flow measurement equation [14] and compared to the case of a homogeneous medium as in the previous study [17]. The considered bubble distribution ensures that the acoustic path is not clear of bubbles when the upstream measurement is simulated.

In case of a homogeneous flowing medium, the clamp-on simulations shown in Figure 6 yield more than 99.6% accuracy, while the in-line simulations shown in Figure 7 are even more precise with 99.8% accuracy. The reason for the better performance of the in-line model is found in the absence of step changes in material parameters between the pipe wall and water causing *Gibbs* oscillations in the clamp-on case. For bubbly flow conditions our simulations predict higher measurement errors, if the standard flow measurement equation is employed. This is because the transit time signal is calculated by cross-correlating up- and donwstream received signals. Such method expects signals of the same envelope which is a reasonable assumption in case of the homogeneous fluid but fails once multiphase flow of high acoustic countrast appears. We see in Figure 6 that our simulations predict up to 40% error, slightly decreasing for higher flow velocities. For the in-line configuration considered in Figure 7, the error is much larger, and is much more difficult to predict. The reason for the difference between the two scenarios lies in the shape of the acoustic beam. The signal frequency $f_c$ is chosen such that a resonance in the pipe wall is achieved [15] so the signal radiates into the fluid over a larger surface, making the flowmeter less sensitive to small shifts in bubble position. This effect is not found in in-line configurations, where the acoustic beam is of comparatively small cross section.

## VI. Conclusion

A goal of this work was to simulate an ultrasonic flowmeter operating under multiphase flow conditions in media of high acoustic impedance contrast. For that purpose a pseudospectral time domain method was developed where scattering from high contrast agents is approximated by directly imposing zero stresses in the areas of the second phase. The method was validated against analytical solutions and showed a good agreement where the main reason for possible mismatches arise from the rasterization of the inclusions. This however only affects the received signal amplitude and not the envelope which is more important in transit time flow measurement. The model was used to demonstrate how a simple cluster of bubbles can result in a complete measurement misreading of the flow rate when the algorithms designed for the homogeneous media are used.

## Acknowledgment

The authors would like to acknowledge support from the *Innovation Fund Denmark* and from the *DeIC National HPC Center* for access to computational resources on *Abacus 2.0*. They would also like to thank Andrei-Alexandru Popa for his help with the experimental measurements.

## References

[1] B. Iooss, C. Lhuillier and H. Jeanneau, Numerical simulation of transit-time ultrasonic flowmeters: uncertainties due to flow profile and fluid turbulence, *Ultrasonics* **40** (2002) 1009-1015.

[2] H. Koechner and A. Mellin, Numerical Simulation of Ultrasonic Flowmeters, *Acustica-acta acustica* **86** (2000) 39-48.

[3] B. Fornberg, High-order finite differences and the pseudospectral method on staggered grids, *SIAM J. Numer. Anal.* **27** (1990) 904-918.

[4] D. V. Mahadeva and R. C. Baker and J. Woodhouse, Studies of the Accuracy of Clamp-on Transit Time Ultrasonic Flowmeters, *IMTC IEEE* (May 2008) 969-973.

[5] M. Bezdek and H. Landes and A. Rieder and R. Lerch, A coupled finite-element, boundary-integral method for simulating ultrasonic flowmeters, *IEEE UFFC* **54** (2007) 639-646.

[6] R. J. LeVeque, *Finite Difference Methods for Ordinary and Partial Differential Equations: Steady-State and Time-Dependent Problems* (SIAM, 2007).

[7] Q. H. Liu, The PSTD algorithm: A time-domain method requiring only two cells per wavelength, *Microwave and Optical Technology Letters* **15** (1997) 158-165. Q. H. Liu

[8] B. A. Auld, *Acoustic Fields and Waves in Solids, Vol. I.* (John Wiley & Sons, 1973).

[9] A. D. Pierce, Wave equation for sound in fluids with unsteady inhomogeneous flow, *J. Acoust. Soc. Am. Vol.* **87** (1990) 2292-2299.

[10] L. N. Trefethen, *Spectral Methods in MATLAB* (SIAM, 2001).

[11] K. C. Meza-Fajardo, A. S. Papageorgiou, A Nonconvolutional, Split-Field, Perfectly Matched Layer for Wave Propagation in Isotropic and Anisotropic Elastic Media: Stability Analysis, *Bulletin of the Seismological Society of America* **98** (2008) 1811-1836.

[12] M. Ghrist, B. Fornberg and T. A. Driscoll, Staggered Time Integrators For Wave Equations, *SIAM J. Numer. Anal.* **38** (2000) 718-741.

[13] F.J. Sanchéz-Sesma, J.A. Peréz-Ruiz and M. Campillo, Elastodynamic 2D Green function retrieval from cross-correlation: Canonical inclusion problem, *Geophysical Research Letters* **33** (2006) L13305.

[14] B. Funck, A. Mitzkus, Acoustic transfer function of the clamp-on flowmeter , *IEEE UFFC* **43** (1996) 569-575.

[15] M.A. Ainslie, Plane-wave reflection and transmission coefficients for a three-layered elastic medium, *J. Acoust. Soc. Am. Vol.* **97** (1995) 954-961.

[16] M. Willatzen, Ultrasound transducer modeling-general theory and applications to ultrasound reciprocal systems, *IEEE UFFC* **48** (2001) 100-112.

[17] M. Simurda, B. Lassen, L. Duggen and N. T. Basse, A Fourier Collocation Approach for Transit-time Ultrasonic Flowmeter under Multi-Phase Flow Conditions, *J. of Computational Acoustics* (2016) Manuscript submitted for publication.